applied sciences

MDPI

Article

Application of Frequency Response Analysis Technique to Detect Transformer Tap Changer Faults

Salem Mgammal Al-Ameri [1], Abdulaziz Almutairi [2,*], Muhammad Saufi Kamarudin [1,*], Mohd Fairouz Mohd Yousof [1,*], Ahmed Abu-Siada [3], Mohamed Ibrahim Mosaad [4] and Saeed Alyami [2]

[1] Department of Power Electrical, Faculty of Electrical and Electronic Engineering, University Tun Hussein Onn Malaysia, 86400 Batu Pahat, Johor, Malaysia; salemawadh@uthm.edu.my
[2] Department of Electrical Engineering, College of Engineering, Majmaah University, AlMajmaah 11952, Saudi Arabia; s.alyami@mu.edu.sa
[3] Electrical and Computer Engineering Department, Curtin University, Bentley, WA 6152, Australia; a.abusiada@curtin.edu.au
[4] Yanbu Industrial College (YIC), Alnahdah, Yanbu Al Sinaiyah, Yanbu 46452, Saudi Arabia; Habibm@rcyci.edu.sa
* Correspondence: ad.almutiri@mu.edu.sa (A.A.); saufi@uthm.edu.my (M.S.K.); fairouz@uthm.edu.my (M.F.M.Y.)

Abstract: Power transformers are located in the electrical transmission and distribution networks where different voltage levels are needed. The turn ratio of the low voltage and high voltage windings is mechanically controlled by an on-load tap changer or de-energized tap changer. As the tap changer is the transformer's only moving part, it is highly susceptible to mechanical failure and aging degradation. While some diagnostic tools have been used to determine the mechanical condition of tap changer contacts, not much attention was given to use the frequency response analysis to diagnose the transformer's tap changers' mechanical integrity. This paper is taking one step forward into maturing the application of the frequency response analysis (FRA) technique to detect transformer tap changer faults. In this regard, two common tap changer faults are created, and experimental testing for four FRA test configurations is conducted. For a better understanding of the tap changer fault mechanism, an electrical equivalent circuit model is proposed and designed using Simulink. The simulation and implementation of the equivalent circuits using MATLAB\R2018a.

Keywords: power transformer; tap changer; coking; pitting; frequency response analysis

Citation: Al-Ameri, S.M.; Almutairi, A.; Kamarudin, M.S.; Yousof, M.F.M.; Abu-Siada, A.; Mosaad, M.I.; Alyami, S. Application of Frequency Response Analysis Technique to Detect Transformer Tap Changer Faults. *Appl. Sci.* **2021**, *11*, 3128. https://doi.org/10.3390/app11073128

Received: 1 March 2021
Accepted: 22 March 2021
Published: 1 April 2021

1. Introduction

Power transformers are vital components in electricity grids and should be maintained in healthy conditions along with their entire operational life. As such several transformer condition monitoring and fault diagnosis techniques have been developed to identify the transformer health condition criticality and its remnant life [1–3]. The tap changer is used in power transformers to adjust the turn's ratio of its windings in order to maintain the voltage at one side at the desired level. This process can be done online through an on-load tap changer (OLTC) or offline using a de-energized tap changer (DETC) [4,5].

The OLTC is an electromechanical system mounted on the transformer to monitor the variable load voltage levels without blocking the load current, while the DETC should shut down the load current before changing the tap manually. This mechanical system is the only moving part in the power transformer and is considered an essential and costly component. The tap changer contacts must be strong enough to withstand regular movement, friction, and mechanical stresses. The tap changer contacts must remain functioning over the transformer's operational lifetime since tap changer replacement is very costly and time-consuming. Around 40–56% of all transformer failures are caused by a tap changer malfunction [6–8]. Tap changer failures may be due to the aging effect due to the electrical, mechanical, thermal, and chemical stresses. The tap changer failure modes comprise of mechanical wear and coking of the contact.

The mechanical stability of the transformer tap changer over its lifetime needs to be assured. There are different tap changer diagnostic methods to assess the tap changer's stability condition that can be classified into oil and insulation analysis, tap changer contact analysis, and mechanical analysis [9]. However, these methods comprise some drawbacks. For instance, dissolved gas analysis (DGA) cannot identify the tap changer damage's exact location. The dynamic resistance measurement (DRM) method can be used to check the tap changer contacts' condition. In this method, a DC power supply is utilized to inject a test voltage into the transformer winding. The vibroacoustic analysis is a new tap changer diagnostic technique that investigates the vibroacoustic waveform transmitted from the tap changer via the structural components to diagnose different tap changer problems [10].

While the frequency response analysis (FRA) technique has been widely used to detect the mechanical deformations of transformer windings and core, not much attention was given to use it for tap changer diagnosis [11,12]. In [13], FRA is used to check its sensitivity to tap changer coking fault. However, the impact of changing the tap position on the FRA signature is investigated. Fundamental analysis for the effect of tap changer coking and pitting on the FRA signature is presented in [14].

Previously, the FRA method is applied for the diagnosis of the transformer core and winding faults. Due to few studies on using the FRA method for tap changer damage detection, this paper presents a further sensitivity analysis of the FRA signature to the transformer tap changer's physical faults. This study implemented faults that include tap changer contacts coking and pitting. The impact of such faults on the FRA signature is investigated through experimental and simulation analyses. Furthermore, the feasibility of using FRA to simultaneously detect winding deformation and tap changer faults is investigated.

The following sections of this work are organized as follows: Section 2 presents the experimental setup, FRA open circuit measurements are introduced in Section 3, FRA short circuit test is expressed in Section 4, capacitive and inductive interwinding tests are presented in Sections 5 and 6 respectively, and final conclusions and recommendations are introduced in Section 7.

2. Experimental Setup

Experimental testing has been conducted on a three-phase 50 Hz, 11/0.415 kV, 500 kVA distribution transformer with a de-energized tap changer. The transformer, windings, and the tap changer configurations are shown in Figure 1 and Table 1. For example, tap 4 and 5 represent Tap1, which selects the whole winding, while Tap5 connects 2 and 7, which only selects the lowest number of turns in the winding.

Table 1. The 11/0.415 kV 500 kVA transformer tap changer configurations.

Tap No.	Input Voltage (kV)	Connected Terminals in Figure 1b
Tap 1	11.550	4, 5
Tap 2	11.275	5, 3
Tap 3	11.000	3, 6
Tap 4	10.725	6, 2
Tap 5	10.450	2, 7

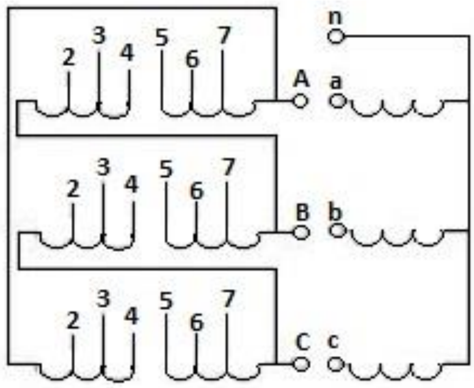

(**a**) (**b**)

Figure 1. (**a**) The 11/0.415 kV, 500 kVA distribution transformer and (**b**) winding configuration.

For the tap changer faults simulation, an arcing switch was represented by 22.5 mm × 30 mm bare copper tape. This conductor was exposed to specific failure modes with real stipulating mechanisms that took place within DETC contacts. Two failure modes, namely, coking and pitting, were applied in the experiment. The FRA was then conducted on the faulty tap changer condition and the tap changer during normal conditions to facilitate comparative analysis. The two implemented faults are elaborated below.

2.1. Coking Formulation

Oil-immersed tap changer is usually subjected to coking process due to the formation of carbonaceous deposits. In a transformer, this process occurs when carbon is extracted from the surrounding transformer oil and deposited on the tap changer contacts due to the heating process during tap position change [15–18]. In this paper, this process was achieved by heating the tap changer contacts to a high-temperature level. The tap changer was immersed in transformer oil over a certain period to form a stipulating condition like practical conditions. Once a carbonaceous deposit film was observed on the contact, experimental FRA measurement was conducted. The polymerized thin oil film reduced the conductivity of the tap changer contact due to its high insulation resistance, which can be detected by FRA. By increasing the thermal stress, more carbonaceous layers will be deposited on the contacts and resulting in higher insulation resistance, as shown in Figure 2.

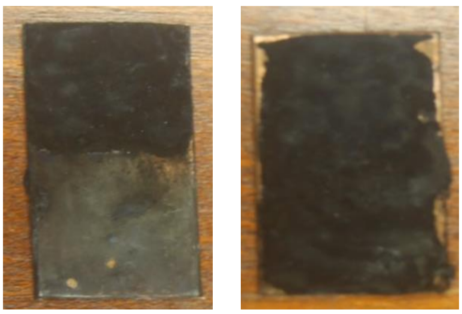

(**a**) (**b**)

Figure 2. Tap contacts coking (**a**) 50% and (**b**) 100%.

2.2. Pitting Formation

Pitting corrosion is formed as cavities in metal materials such as copper. This type of fault is considered to be more harmful and is hard to diagnose [19]. In this paper, pitting of different levels on the copper surface was achieved using mechanical tools. The resultant copper tape with 50% and 100% pitting was as illustrated in Figure 3.

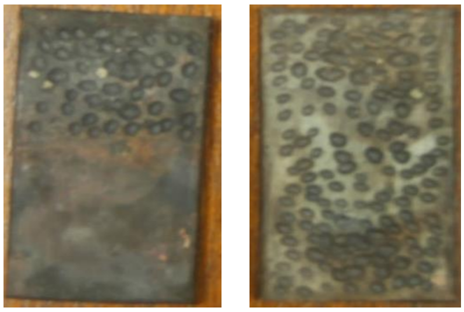

(**a**) (**b**)

Figure 3. Tap surface pitting (**a**) 50% and (**b**) 100%.

3. FRA Open Circuit Measurement

End to end open circuit FRA measurement was performed using a commercial frequency response analyzer by injecting 20 V input voltage signal (V_i) of low amplitude and variable frequency to one terminal of the HV winding and measuring the output voltage (V_o) at the other end of the same winding while all LV windings are left open [7]. The FRA signature was plotted at all tap positions as the winding transfer function (V_o/V_i) in dB, as shown in Figure 4.

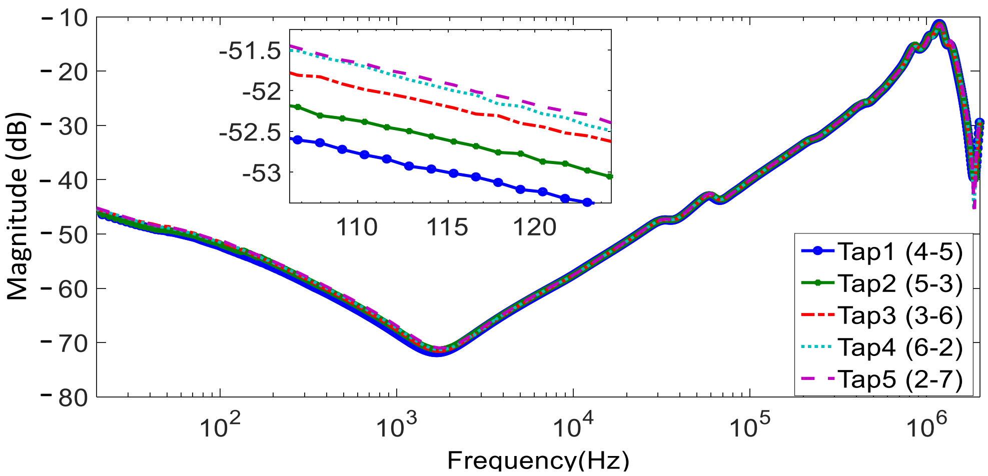

Figure 4. Measured frequency response analysis (FRA) at all tap changer positions.

According to [20], the FRA technique can be developed based on the fact that transformer components can be presented by a complex network of a distributed resistance R, inductance L, capacitance C, and conductance G parameters. In [21,22], the equivalent circuit of the transformer considered the series and paralleled resistance, inductance, and capacitance RLC elements are presented, as shown in Figure 5. Where n is the number of disc. In this study, a new simplified circuit model was proposed to simulate the measured transformer FRA. Hence, the proposed lumped RLC circuit model in Figure 6 represented the transformer in a normal tap changer at the end-to-end open circuit measurement. The R_s and L_s, refers to series resistance and inductance, and C_p is the primary capacitance. Each wire resistance R and reference resistance R_{ref} were 50 Ω.

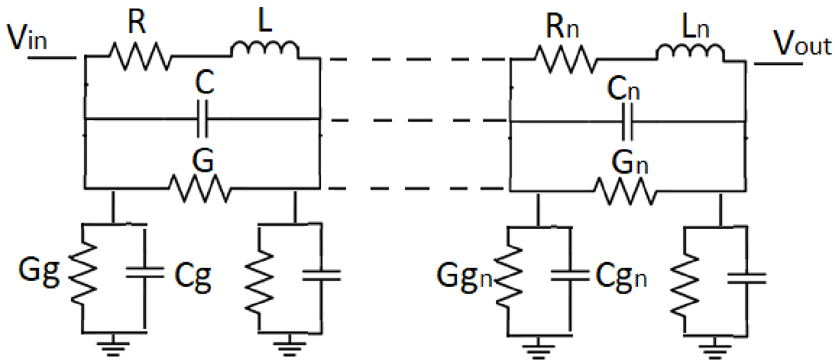

Figure 5. Equivalent schematic resistance, inductance, and capacitance RLC network of transformer winding.

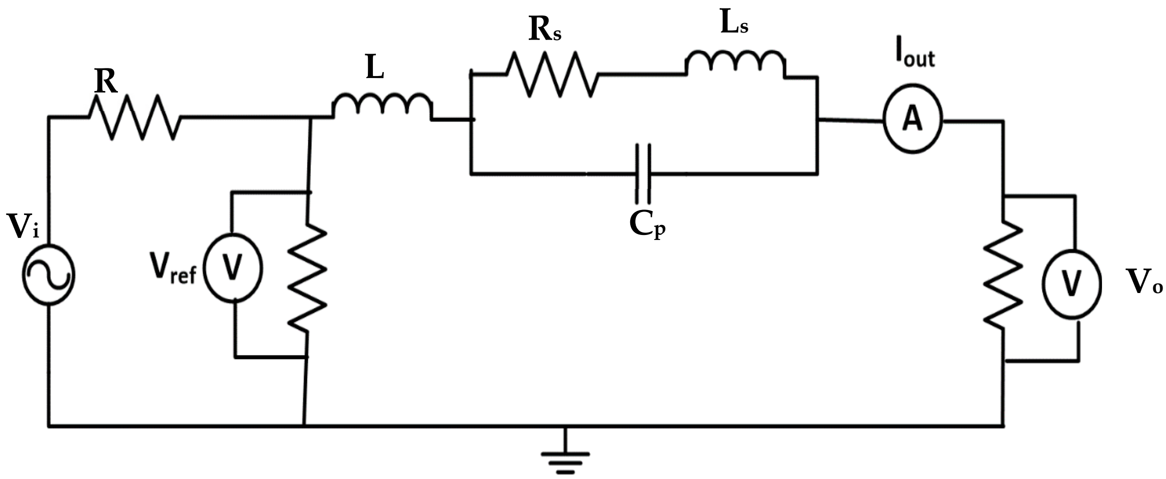

Figure 6. Simulated tap changer RLC circuit using MATLAB/Simulink.

The parameters of the transformer equivalent circuit shown in Figure 6 obtained through finite element analysis simulation to the investigated transformer using its physical dimensions, insulation properties, and winding topology as detailed in [23–25]. These parameters are given in Table 2.

Table 2. RLC circuit parameters for the tap changer at different positions for the FRA open circuit test.

Tap Position	L (μH)	R_s Ω	L_s (μH)	C_p (pF)
Tap 4–5	5.00	1	100	100
Tap 5–3	4.75	1.5	110	95
Tap 3–6	4.50	1.10	120	90
Tap 6–2	4.25	1.15	130	85
Tap 2–7	4.00	1.20	140	80

Figure 4 shows that FRA signatures for all tap settings in normal tap conditions had a similar trend with the same resonance frequencies but slight changes in the transfer function's magnitude. The leakage and magnetizing inductances of the core affected the FRA at low frequency (below 2 kHz), which begins with the decreasing magnitude of −20 dB/decade under normal tap changer contacts. At the mid-frequency range, resonances appeared intermittently due to parasitic capacitances and inductances of the transformer. At higher frequencies above 1 MHz, the transformer structure affected the signature. The connection leads and measurement setups were taken into this high-frequency range.

The FRA of the proposed lumped RLC model was plotted at the same tap positions by changing the RLC values shown in Figure 7, which shows a similar profile to the measured signatures shown in Figure 5. The slight change in the transfer function magnitude from a tap position to another was attributed to the change in the equivalent electrical parameters. However, the location of resonance frequencies was not changing.

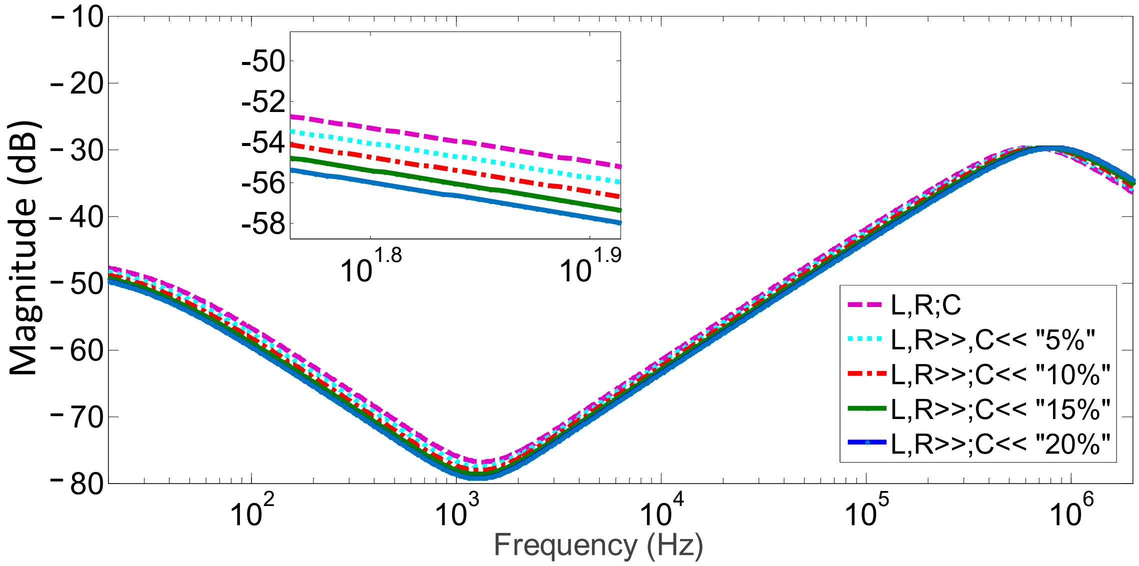

Figure 7. Simulated FRA for at all tap changer positions.

3.1. Measured and Simulated FRA Signature for Normal vs. Coking Taps

Figure 8 shows the measured FRA signature for 50% and 100% tap contacts coking along with the normal condition FRA signature. It can be seen that there was a dramatic reduction in the FRA signature due to the tap changer coking contact at the low-frequency region, 20 Hz to 2 kHz. This effect was attributed to the increase in the tap resistance due to coking, as explained above. This effect could be simulated by changing the equivalent circuit parameters, as shown in Table 3. The parameters were obtained through finite element analysis simulation to the investigated transformer using its physical dimensions, insulation properties, and winding topology as detailed in [23–25]. The measured and simulated FRA signatures are plotted as shown in Figures 8 and 9, which revealed a similar trend for both. Thus, the RLC model could better understand the effect of tap changer faults on the FRA signature. It can be seen that, while the series resistance was significantly increasing due to coking, the capacitive and inductive components were almost constant, as shown in Table 3. This explains the signature magnitude changes, particularly in the low-frequency range without an observable change in the resonance frequencies. A slight variation can be observed by comparing coking at different levels of degradation severity (50% and 100% coking) (Figure 8). This variation at the low-frequency range was due to increased resistance of the contacts with more deposited oil film layers. However, at the high frequencies range, the winding structure influenced the frequency response and made a rising trend in the signature due to the winding structure's high capacitance.

Table 3. Simulated RLC model parametric values for normal and coking.

Condition	L (µH)	Ls (µH)	Rs Ω	Cp (pF)
Normal	5	1	1	0.593
Coking 50%	5	0.909	100	0.538
Coking 100%	5	0.909	110	0.538

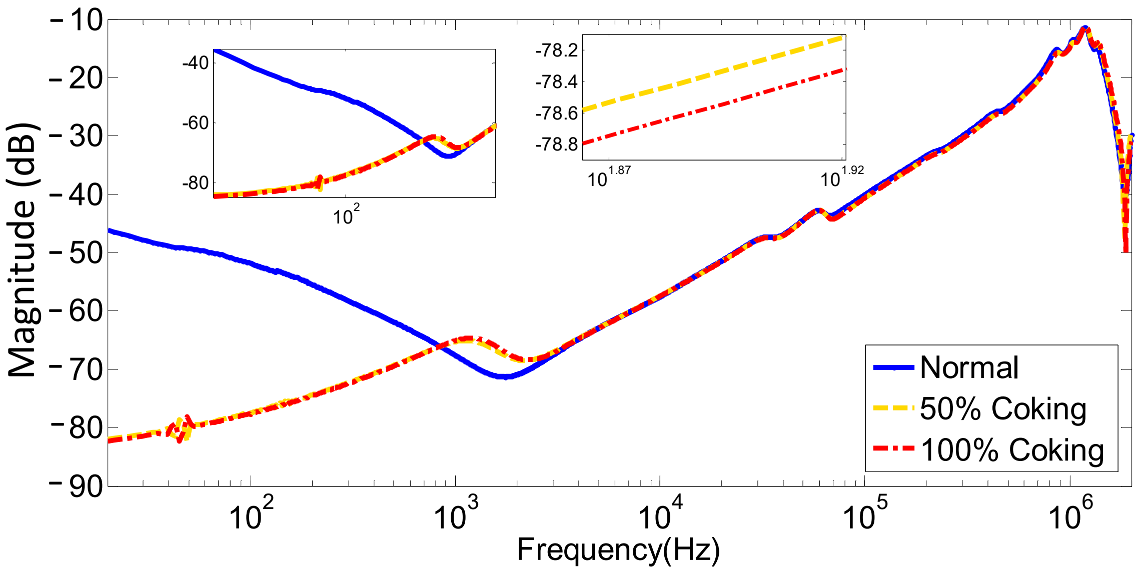

Figure 8. Measured FRA for normal, 50%, and 100% coking.

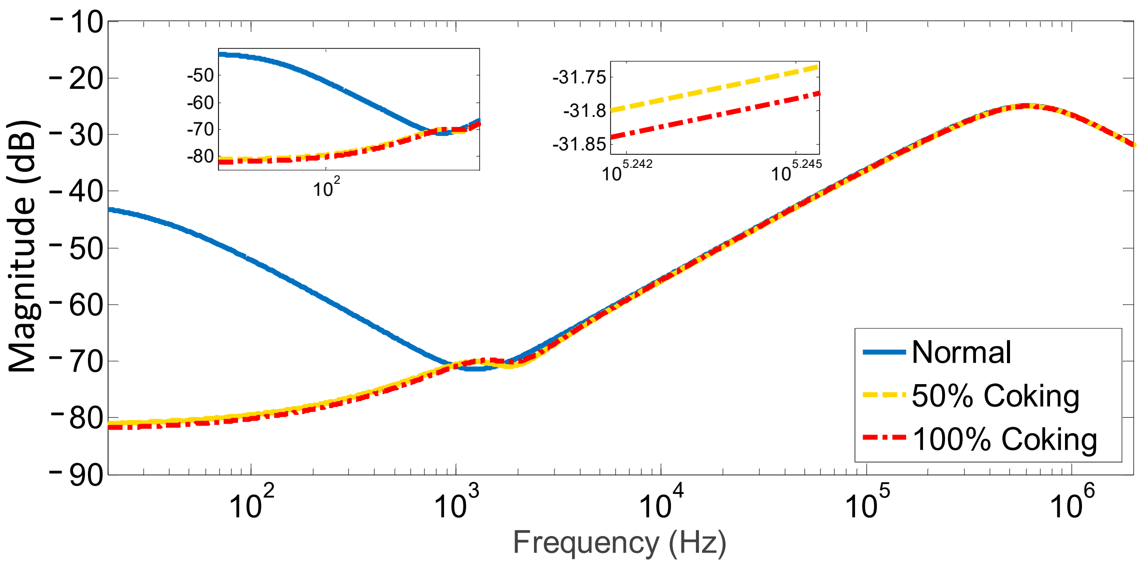

Figure 9. Simulated FRA for normal, vs. 50% and 100% coking.

3.2. Measured and Simulated FRA for Normal vs. Pitting

Naturally, pitting or contact wear occurs due to the mechanical stress on the contact's surface during load transfers. This degradation affected the normal tap changer accompanied by coking. Unlike other defects, pitting on the arcing switch contact surface seemed to have no significant impact on the FRA measurements. Since pitting reduces the contact surface area, it results in increased resistance [11], although other research findings show a reduction in the resistance value using the dynamic resistance measurement [9,12]. Pitting probably occurs due to the copper conductor's compaction of chemical properties, which causes more free electrons to flow in the conductor, thus increasing the conductivity. However, a further investigation is required to evaluate the cause of resistance reduction in pitting conditions. The measured and simulated FRA signatures due to pitting are presented in Figures 10 and 11, respectively. A simulated FRA signature during pitting condition was obtained using the circuit parameters listed in Table 4.

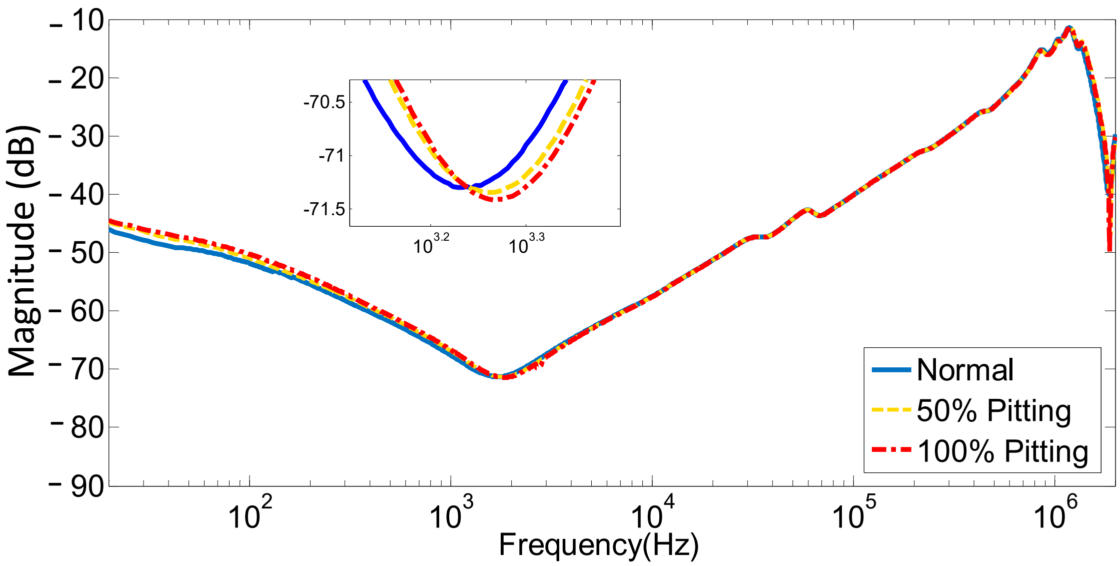

Figure 10. Measured FRA for normal, vs. 50% and 100% pitting.

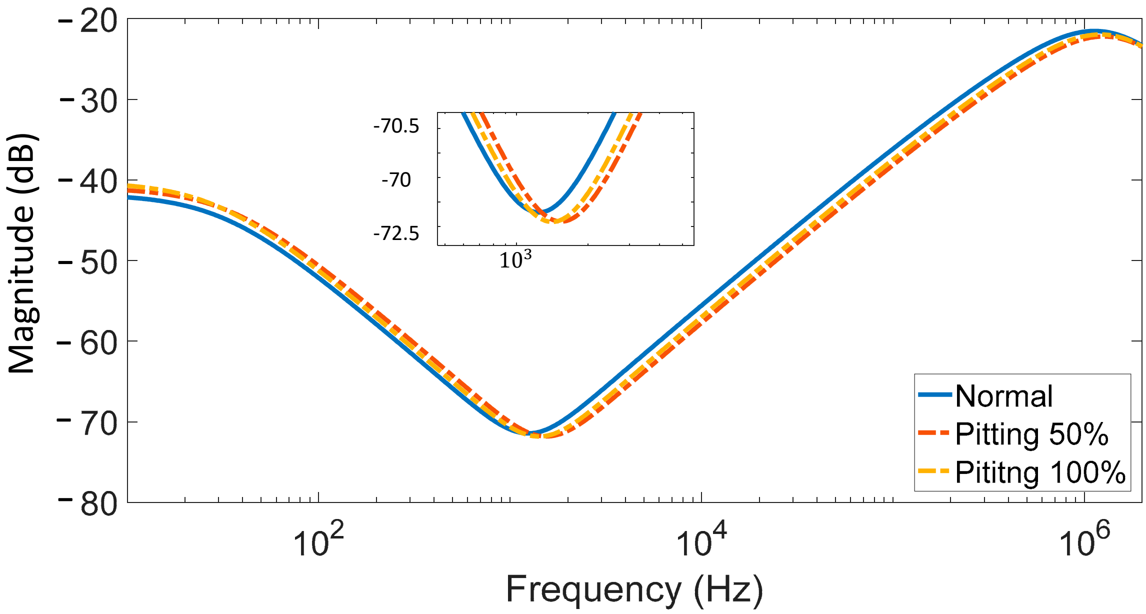

Figure 11. Simulated FRA for normal, vs. 50% pitting and 100% pitting.

Table 4. Values of a simulated circuit model for pitting.

Condition	L (μH)	Ls (μH)	Rs Ω	Cp (pF)
Normal	500	0.001	1	0.512
Pitting 50%	500	0.002	909.1	0.464
Pitting 100%	500	0.003	833.3	0.464

Results in Figures 10 and 11 show a slight variation in the FRA signature due to contact pitting. At the low-frequency region and due to pitting, the FRA signature tended to shift upward when compared with the normal condition due to the reduction in resistance and inductance values. At the mid and high frequency ranges, the FRA response tended to shift downward due to a decrease in the capacitance value. According to the degree of severity, it can be shown that at 100% pitting, the signature exhibited a higher shift than the 50% pitting, which was attributed to their effects on the resistive and capacitive components.

4. FRA Short Circuit Test

This test was conducted similar to the above case study but with the low voltage windings shorted together to eliminate the effect of the magnetizing inductance of the magnetic core. This configuration can be modeled using the equivalent circuit shown in Figure 12 with the parameters listed in Table 5 [7]. The proposed lumped RLC circuit model represented the transformer at normal, coking, and pitting at the end-to-end short circuit measurement.

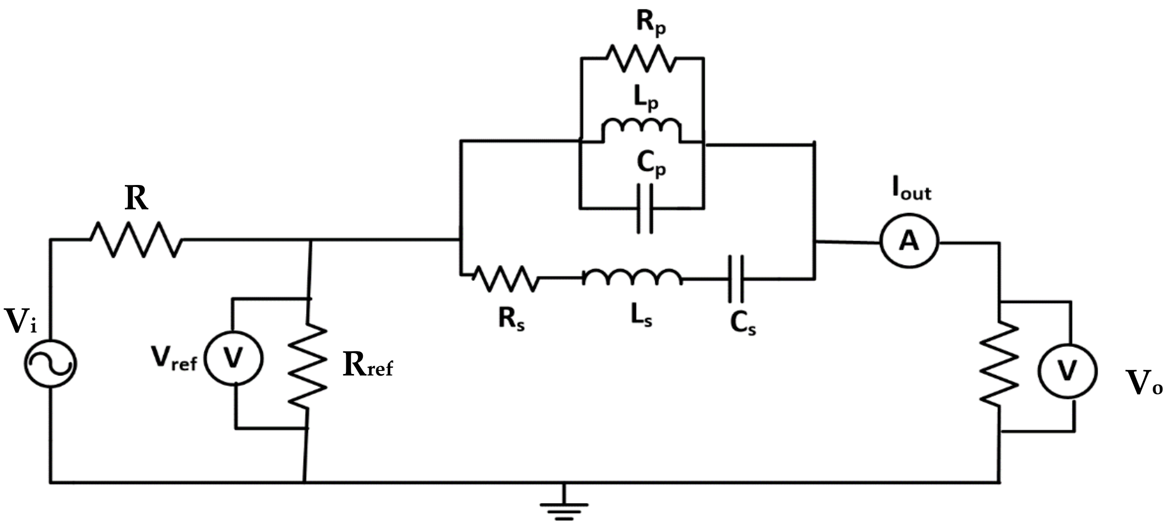

Figure 12. The RLC circuit model for the tap changer under the FRA short circuit test.

Table 5. Values of simulated short circuit model parameters.

Condition	Lp (mH)	Cp (pF)	Rs Ω	Ls (mH)	Cs (nF)
Normal	1	0.10	1	100	1.12
Pitting	1	0.10	1000	100	1.12
Coking	1	0.83	1000	50	1.01

The measured and simulated FRA signatures for this configuration under coking and pitting conditions of different levels are shown in Figures 13 and 14, respectively. For the normal signature, the resonance frequencies were shifted toward a higher range due to the absence of a transformer core effect. The low and mid frequency regions' response was dominated by the leakage inductance and was characterized by a negative slope. At higher frequencies, the transformer was considered purely capacitive, and the response was approximately similar for the investigated cases shown in both figures.

Figures 13 and 14 revealed a significant effect of the tap changer contact coking on the FRA signature in the low and mid-frequency ranges. This effect occurred due to the increment of transformer leakage inductance and the reduction in the winding resistance. Additionally, the resonance frequency was shifted towards higher frequencies due to the decrease in the magnetizing impedance. On the other hand, pitting shows no variation in the FRA signature at low frequencies. However, a hardly observable deviation in the FRA curve occurred at higher frequencies because of the slight reduction in the series and ground capacitances with no deviation in the resonance frequency.

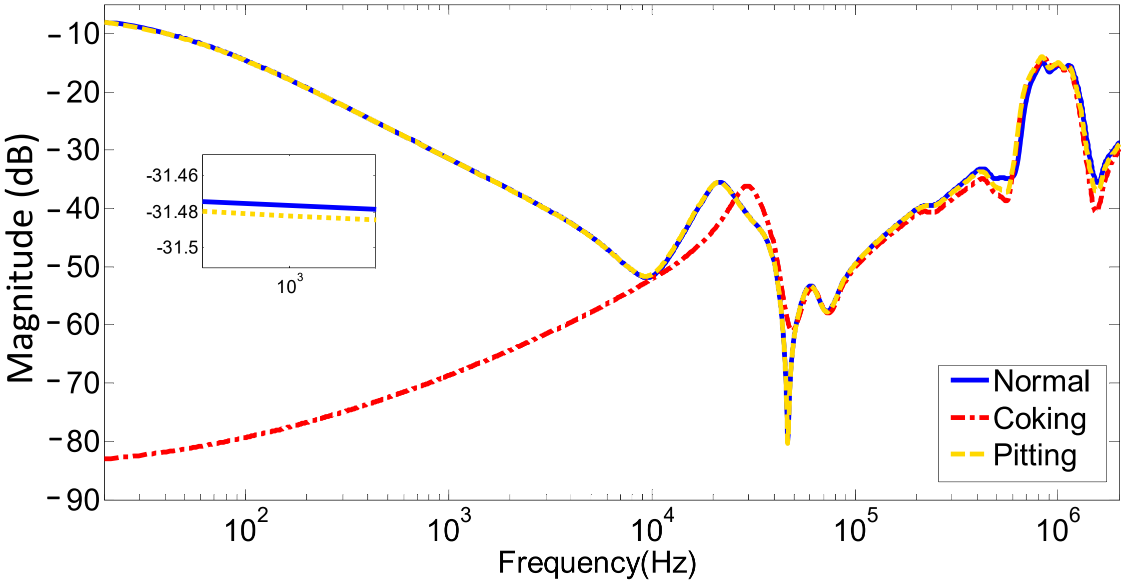

Figure 13. Measured FRA for normal, vs. 100% coking and 100% pitting.

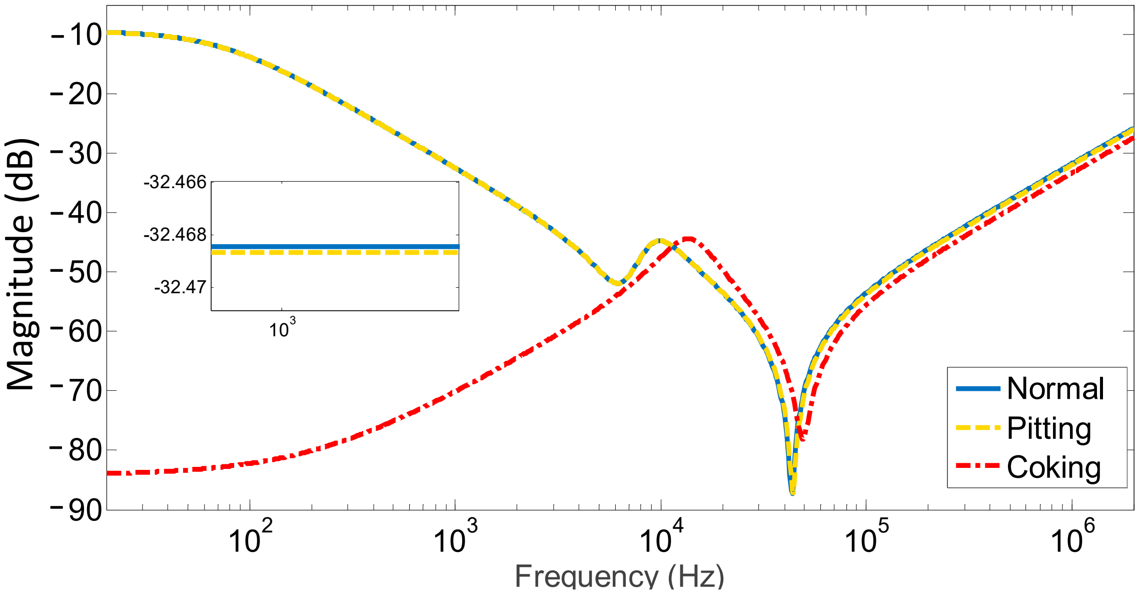

Figure 14. Simulated FRA for normal, vs. 100% coking and 100% pitting.

5. Capacitive Interwinding Test

In the capacitive interwinding test, the input signal was injected at one terminal of the high voltage winding, and the response was measured at the end of the low voltage winding on the same phase, while the terminals of other windings were kept floating [7]. Measured response is shown in Figure 15. The simulated FRA responses, obtained using the circuit model shown in Figure 16. The proposed simplified capacitive lumped RLC circuit model represented the transformer at normal, coking, pitting at the capacitive interwinding measurement. This configuration measured and simulated responses are presented in Figures 15 and 17. In Figure 15, the frequency response was highly capacitive, revealed by the increment of magnitude due to the very high impedance, which results in a plot beginning at a low dB value. There was a significant difference in the frequency response at low frequencies, particularly from 20 to 1 kHz. The coking caused an increase in the contact's impedance, which results in the plot beginning at very low dB. This gradual increase exhibited the dominant influence of the inter-winding capacitance of the power transformer. The model of the transformer was used in conjunction with the analysis of interwinding capacitances. There was a good agreement between simulated and measured FRA signatures. Results show that coking affected the response at the low-frequency range by reducing its magnitude while the effect of pitting was not visibly observed. The resistance and inductance of tap contacts show no significant impact on the response due to the domination of the interwinding capacitance that is listed in Table 6.

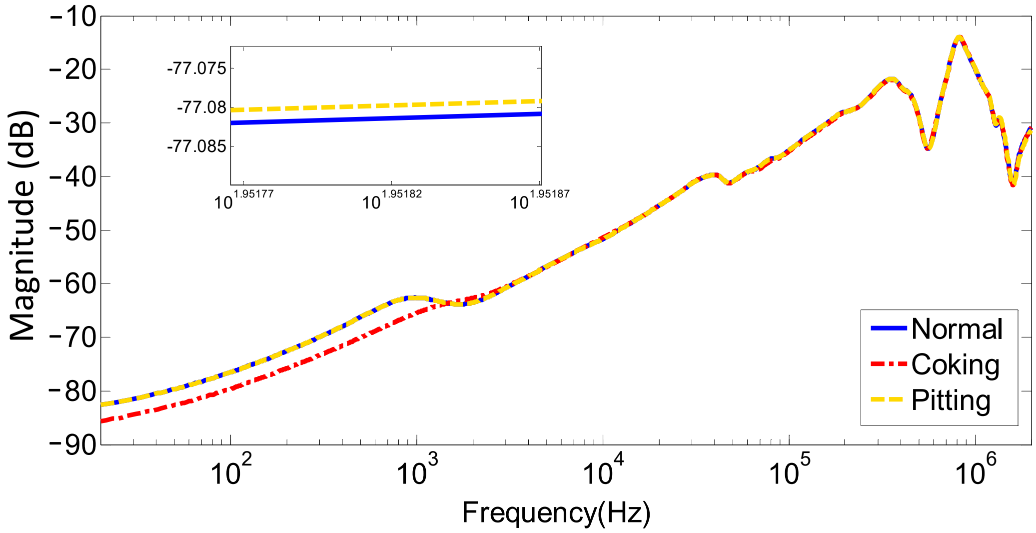

Figure 15. Measured capacitive interwinding FRA for normal vs. 100% coking and 100% pitting tap conditions.

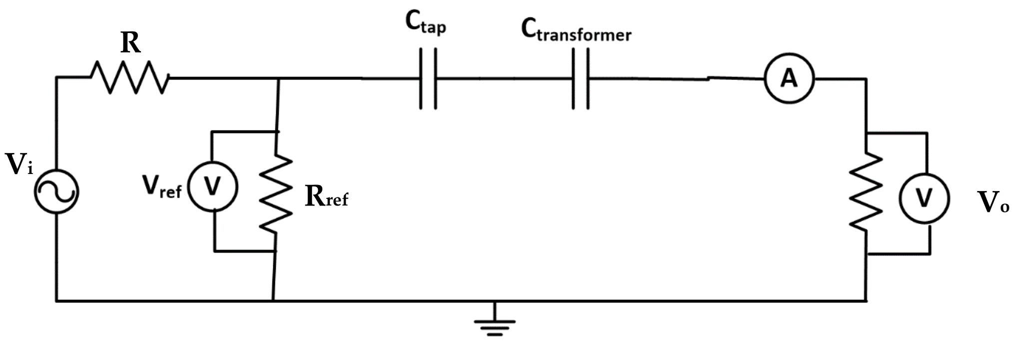

Figure 16. Capacitive interwinding test configuration.

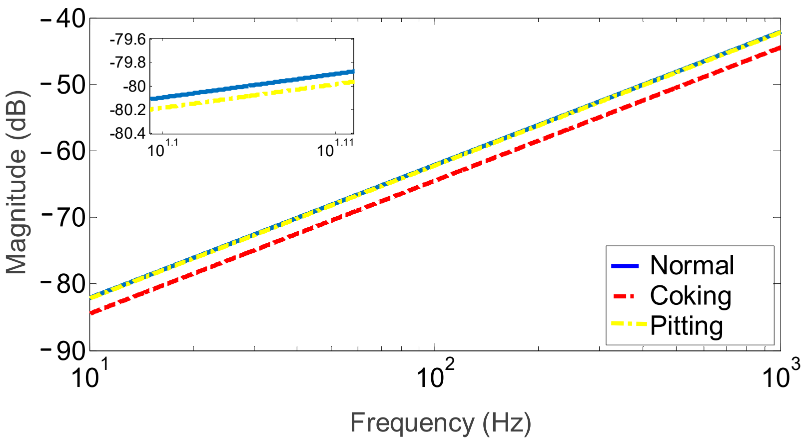

Figure 17. Simulated capacitive interwinding FRA for normal vs. 100% coking and 100% pitting tap conditions.

Table 6. Capacitive intertwining value of different conditions.

Condition	Interwinding Capacitance (μF)
Normal	0.05
Pitting	0.0495
Coking	0.0381

6. Inductive Interwinding Test

In the inductive interwinding test, the input signal was applied at one terminal of the HV winding, and the output signal was measured at the terminal of the LV winding of the same phase [7]. The proposed simplified inductive lumped RLC circuit model represented the transformer at normal, coking, pitting at the inductive interwinding measurement. The circuit model is shown in Figure 18 with parameters listed in Table 7. The other HV and LV terminals are connected to the ground. The FRA plots for normal and faulty tap conditions are presented in Figure 19.

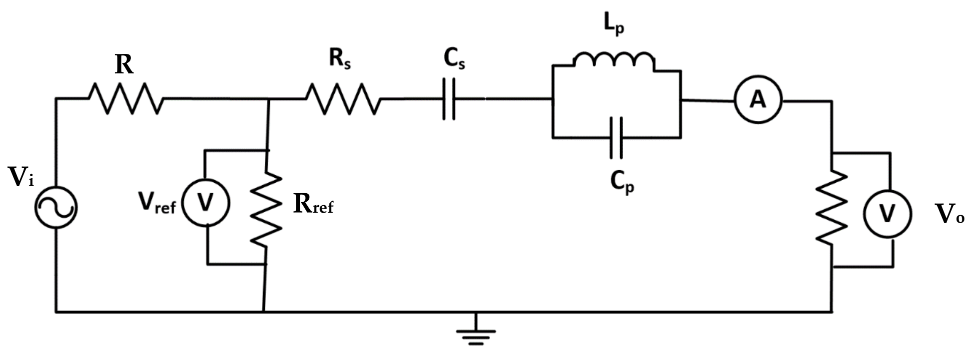

Figure 18. Inductive interwinding test configuration.

Table 7. Values of simulated short circuit model parameters.

Condition	Lp (mH)	Cp (μF)	Rs Ω	Cs (μF)
Normal	1	1	2	2000
Pitting	1	1.5	2380	0.0202
Coking	1	1.27	2380	0.0263

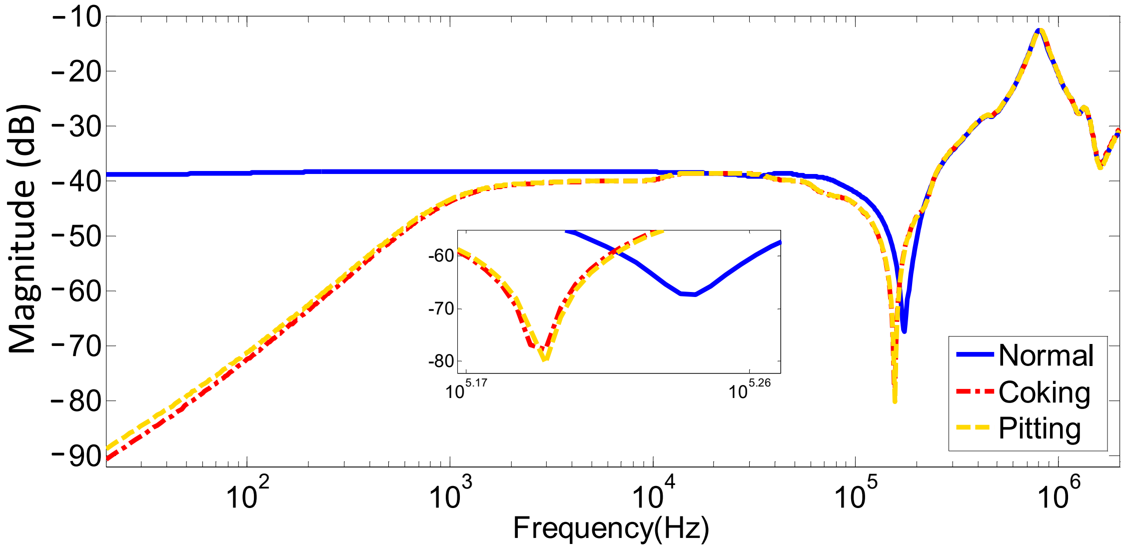

Figure 19. Measured FRA for normal, 100% coking, and 100% pitting.

In normal conditions, the FRA signature starts with a constant magnitude due to the absence of the mutual inductances. The winding structure influences the region between 100 kHz and 1 MHz, in which the response was affected by leakage inductance together with the winding series and ground capacitances. In this region, the series capacitance is the most influential factor in determining the response's shape as a generic rising amplitude with few resonance frequencies, while the connection leads effect occurred at higher frequencies (>1 MHz). The FRA signatures obtained from the simulation model for different tap changer conditions are shown in Figure 20.

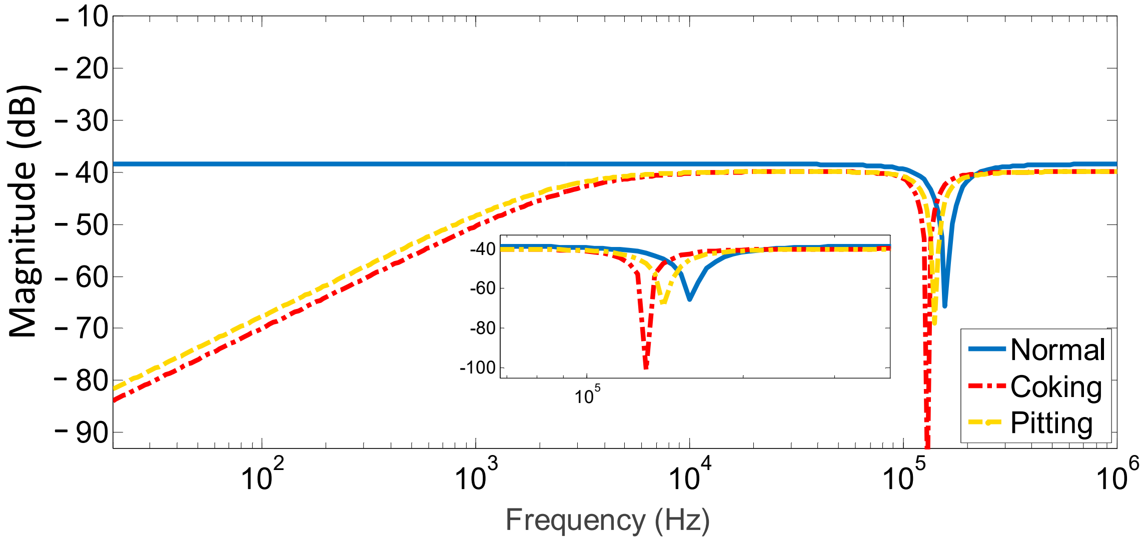

Figure 20. Simulated FRA for normal, vs. 100% coking and 100% pitting.

Like the measured FRA signatures, Figure 20 indicates a significant reduction in the transfer function's amplitude in the frequency range 20 Hz to 3 kHz for both types of faults. For both faults, the slight increase in the resistance contributes to reducing FRA signature toward negative magnitude. However, there is a drastic decrease in transformer capacitance, which causes the frequency slope to shift towards low magnitudes in the low-frequency region. There was also a slight shift in the frequency response toward the low frequencies, as shown in the inset plot in Figure 20. This shift occurred due to the increase in transformer shunt capacitance.

7. Conclusions

In this paper, an attempt was made to evaluate the effect of degraded tap changer contacts on the transformer FRA signature. Obtained experimental and simulation results revealed the feasibility of using FRA measurement to identify various contact faults such as coking and pitting. While coking had an observable effect on the FRA signatures obtained using different measurement configurations, the impact of pitting fault was only visually observed in the inductive interwinding configuration. The effects of these faults on the FRA signatures were explained through the proposed RLC equivalent circuit model. The shift of the signature in the low-frequency range due to contact faults could be used as an indicator for the detection of degraded tap contacts, and the amount of change could be correlated to the severity of fault level. Results also show that open circuit, short circuit, and inductive interwinding give some FRA variations due to both faults at the low frequency range, while capacitive interwinding was not effective to evacuate the tap contacts degradations, especially for affected contacts due to sliding mechanical stress (pitting). The inductive interwinding test configuration is a more useful test configuration for diagnosing transformer tap contact degradation, including pitting, which is hardly observable in other connection setups.

Author Contributions: Conceptualization, S.M.A.-A. and M.F.M.Y.; methodology, S.M.A.-A., A.A., M.F.M.Y. and M.S.K.; software, S.M.A.-A. and M.F.M.Y.; validation, S.M.A.-A., A.A.-S., S.A. and M.F.M.Y.; investigation, S.M.A.-A., M.F.M.Y. and M.S.K.; resources, S.M.A.-A. and M.F.M.Y.; writing—original draft preparation, S.M.A.-A. and M.F.M.Y.; writing review and editing, M.F.M.Y., A.A., M.S.K., A.A.-S., M.I.M. and S.A.; Project administration: M.F.M.Y., M.I.M., A.A. and M.S.K. All authors have read and agreed to the published version of the manuscript.

Funding: This work was supported by the Deanship of Scientific Research, Majmaah University, under Grant NO. R-2021-71.

Institutional Review Board Statement: Not applicable.

Informed Consent Statement: Informed consent was obtained from all subjects involved in the study.

Data Availability Statement: The data presented in this study are available in this article.

Acknowledgments: The authors extend their appreciation to the Deputyship for Scientific Research, Majmaah University, for funding this research work through project number (Grant NO. R-2021-71). The authors would like to thank M. A. Talib from TNBR Malaysia for his assistance during the experiment. We would also like to thank all the subjects who volunteered to participate in this study.

Conflicts of Interest: The authors declare no conflict of interest.

References

1. Banaszak, S.; Szoka, W. Cross Test Comparison in Transformer Windings Frequency Response Analysis. *Energies* **2018**, *11*, 1349. [CrossRef]
2. Abu-Siada, A.; Arshad, M.; Islam, S. Fuzzy Logic Approach to Identify Transformer Criticality using Dissolved Gas Analysis. In Proceedings of the 2010 IEEE PES General Meeting, Minneapolis, MN, USA, 25–29 July 2010. [CrossRef]
3. Shang, R.; Peng, C.; Fang, R. A Segmented Preprocessing Method for the Vibration Signal of an On-Load Tap Changer. *Electronics* **2021**, *10*, 131. [CrossRef]
4. Abu-Siada, A.; Islam, S. Adaptive Setting of OLTC to Improve Power Transfer Capability of Power Systems. In Proceedings of the 2008 International Conference on Condition Monitoring and Diagnosis, CMD'08, Beijing, China, 21–24 April 2008. [CrossRef]
5. Abu-Siada, A.; Islam, S.; Mohamed, E.A. Application of Artificial Neural Networks to Improve Power Transfer Capability through OLTC. *Int. J. Eng. Sci. Technol. (IJEST)* **2010**, *2*, 8–18. [CrossRef]
6. del Nozal, Á.; Romero-Ramos, E.; Trigo-García, Á. Accurate Assessment of Decoupled OLTC Transformers to Optimize the Operation of Low-Voltage Networks. *Energies* **2019**, *12*, 2173. [CrossRef]
7. IEC 60076-18 Ed.1. Power Transformers—Part 18, 'Measurement of Frequency Response'. 2012. Available online: https://webstore.iec.ch/publication/597 (accessed on 2 December 2020).
8. Yang, R.; Zhang, D.; Li, Z.; Yang, K.; Mo, S.; Li, L. Mechanical Fault Diagnostics of Power Transformer On-Load Tap Changers Using Dynamic Time Warping. *IEEE Trans. Instrum. Meas.* **2019**, 68. [CrossRef]
9. Aziz, M.A.A.; Talib, M.A.; Arumugam, R. Diagnosis of On-Load Tap Changer (OLTC) using dynamic resistance measurement. In Proceedings of the 2014 IEEE 8th International Power Engineering and Optimization Conference (PEOCO2014), Langkawi, Malaysia, 24–25 March 2014; pp. 494–497. [CrossRef]
10. Liu, J.; Wang, G.; Zhao, T.; Zhang, L. Fault Diagnosis of On-Load Tap-Changer Based on Variational Mode Decomposition and Relevance Vector Machine. *Energies* **2017**, *10*, 946. [CrossRef]
11. Yousof, M.F.M.; Al-Ameri, S.; Ahmad, H.; Illias, H.A.; Arshad, S.N.M. A New Approach for Estimating Insulation Condition of Field Transformers Using FRA. *Adv. Elect. Comp. Eng.* **2020**, *20*, 35–42. [CrossRef]
12. Yousof, M.F.M.; Ekanayake, C.; Saha, T.K. An investigation on the influence of tap changer on Frequency Response Analysis. In Proceedings of the 2015 IEEE 11th International Conference on the Properties and Applications of Dielectric Materials (ICPADM), Sydney, Australia, 19–22 July 2015; Volume 2015, pp. 963–966. [CrossRef]
13. Erbrink, J.; Smit, J.; Gulski, E.; Leich, R. Experimental model for diagnosing on-load tap changer contact aging with dynamic resistance measurements. In Proceedings of the CIRED 2009—The 20th International Conference and Exhibition on Electricity Distribution, Prague, Czech Republic, 8–11 June 2009; pp. 1–4. [CrossRef]
14. Al-Ameri, S.; Yousof, M.F.M.; Ahmad, H.; Alsubari, M.; Talib, M.A. Examining Faulty Transformer Tap Changer using Frequency Response Analysis. *Int. Symp. Electr. Insul. Mater. (ISEIM)* **2017**, 259–262. [CrossRef]
15. Al-Ameri, S.; Alawady, A.A.M.; Yousof, M.F.M.; Ahmad, H.; Salem, A.A.A.; Talib, M.A. Frequency response analysis for transformer tap changer damage detection. *Int. J. Power Electron. Drive Syst.* **2020**, *11*, 350–358. [CrossRef]
16. Hillergren, J.; Lindahl, M. On Moving Contacts in On-Load Tap Changers. Master's Thesis, Chalmers University of Technology, Göteborg, Sweden, 2010. Available online: https://publications.lib.chalmers.se/records/fulltext/128506.pdf (accessed on 25 December 2020).

17. Erbrink, J.J.; Gulski, E.; Smit, J.J.; Seitz, P.P.; Leich, R. Experimental model of aging mechanisms of on-load tap changer contacts. In Proceedings of the International Conference on Condition Monitoring and Diagnosis, Beijing, China, 21–24 April 2008; pp. 247–250. [CrossRef]
18. Bustamante, S.; Manana, M.; Arroyo, A.; Laso, A.; Martinez, R. Determination of Transformer Oil Contamination from the OLTC Gases in the Power Transformers of a Distribution System Operator. *Appl. Sci.* **2020**, *10*, 8897. [CrossRef]
19. Banaszak, S.; Szoka, W. Influence of a Tap Changer Position on the Transformer's Frequency Response. In Proceedings of the Innovative Materials and Technologies in Electrical Engineering (i-MITEL), Sulęcin, Poland, 18–20 April 2018. [CrossRef]
20. Banaszak, S.; Gawrylczyk, K.M.; Trela, K. Frequency response modelling of transformer windings connected in parallel. *Energies* **2020**, *13*, 1395. [CrossRef]
21. Banaszak, S.; Gawrylczyk, K.M. Computer modeling in the diagnostics of transformers' windings deformations. *Comput. Appl. Electr. Eng.* **2020**, *8*, 132–140. Available online: https://yadda.icm.edu.pl/baztech/element/bwmeta1.element.baztech-1795d009-9db1-4052-b34d-e607246d589e (accessed on 17 March 2021).
22. Al-Ameri, S.; Yousof, M.F.M.; Azis, N.; Avinash, S.; Talib, M.A.; Salem, A.A. Frequency response of transformer winding to investigate the influence of RLC. *Indones. J. Electr. Eng. Comput. Sci.* **2019**, *14*, 219–229. [CrossRef]
23. Abu-Siada, A.; Mosaad, M.I.; Kim, D.; El-Naggar, M.F. Estimating Power Transformer High Frequency Model Parameters Using Frequency Response Analysis. *IEEE Trans. Power Deliv.* **2020**, *35*, 126–1277. [CrossRef]
24. Aljohani, O.; Abu-Siada, A. Application of Digital Image Processing to Detect Transformer Bushing Faults and Oil Degradation using FRA Polar Plot Signature. *IEEE Trans. Dielectr. Electr. Insul.* **2017**, *24*, 428–436. [CrossRef]
25. Abu-Siada, A.; Aljohani, O. Detecting Incipient Radial Deformations of Power Transformer Windings using Polar plot and Digital Image Processing. *IET Sci. Meas. Technol.* **2018**, *12*, 492–499. [CrossRef]